Strongly Altered Receptor Binding Properties in PP and NPY Chimeras Are Accompanied by Changes in Structure and Membrane Binding[†,‡]

Mirjam Lerch,[§,||] Hiroshi Kamimori,[⊥,#] Gerd Folkers,[§,▽] Marie-Isabel Aguilar,[⊥,○] Annette G. Beck-Sickinger,[◇] and Oliver Zerbe*[,§,¥]

Institute of Pharmaceutical Sciences, ETH Zurich, Switzerland, Institute of Molecular Biology and Biochemistry, Monash University, Australia, Institute of Biochemistry, University of Leipzig, Germany, and Institute of Organic Chemistry, University of Zurich, Winterthurerstrasse 190, CH-8057 Zurich, Switzerland

Received January 21, 2005; Revised Manuscript Received May 3, 2005

ABSTRACT: Neuropeptide Y (NPY) and the pancreatic polypeptide (PP) are members of the neuropeptide Y family of hormones. They bind to the Y receptors with very different affinities: Whereas PP is highly selective for the Y_4 receptor, NPY displays highest affinites for Y_1, Y_2, and Y_5 receptor subtypes. Introducing the NPY segment 19−23 into PP leads to an increase in affinity at the Y_1 and Y_2 receptor subtypes whereas the exchange of this segment from PP into NPY leads to a large decrease in affinity at all receptor subtypes. PP displays a very stable structure in solution, with the N terminus being back-folded onto the C-terminal α-helix (the so-called PP-fold). The helix of NPY is less stable and the N terminus is freely diffusing in solution. The exchange of this segment, however, does not alter the PP-fold propensities of the chimeric peptides in solution. The structures of the phospholipid micelle-bound peptides serving to mimic the membrane-bound species display segregation into a more flexible N-terminal region and a well-defined α-helical region. The introduction of the [19−23]-pNPY segment into hPP leads to an N-terminal extension of the α-helix, now starting at Pro^{14} instead of Met^{17}. In contrast, a truncated helix is observed in [$^{19-23}$hPP]-pNPY, starting at Leu^{17} instead of Ala^{14}. All peptides display moderate binding affinities to neutral membranes (K_{assoc} in the range of 1.7 to 6.8 × 10^4 mol^{-1} as determined by surface plasmon resonance) with the differences in binding being most probably related to the exchange of Arg-19 (pNPY) by Glu-23 (hPP). Differences in receptor binding properties between the chimeras and their parental peptides are therefore most likely due to changes in the conformation of the micelle-bound peptides.

Neurohormones play an important role in the regulation of numerous biological processes. The neuropeptide Y (NPY[1]) family of neuroendocrinic peptides includes the neurotransmitter NPY and the two gut hormones peptide YY (PYY) and pancreatic polypeptide (PP). These peptides contain 36 residues and are C-terminally amidated. The sequences of the peptides discussed in this study are listed in Table 1. They activate the so-called Y receptors, six subtypes of which have been characterized so far and are called Y_1−y_6 receptors (*1*). They are G_i-protein coupled receptors, and upon activation they inhibit adenylate cyclase and lead to increased levels of intracellular calcium.

PP is mainly expressed in the endocrinic pancreas and is released as a response to food intake (*2*). It acts as a regulator of feeding behavior (*3*). PP binds with picomolar affinity to the Y_4 receptor and with nanomolar affinity to the Y_5 receptor. The binding affinities are given in Table 2. NPY is localized in neurons of various regions of the brain as well as in peripheral neurons. NPY is also important for the regulation of food intake and is involved in the regulation of various physiological processes. It exhibits subnanomolar affinities to the Y_1, Y_2, and Y_5 receptors and low nanomolar affinities to the Y_4 receptor (see Table 2). For a recent review on the NPY family see Mörl et al. (*4*).

[†] We acknowledge financial support from the TH fund from the ETH Zurich to M.L. (TH Grant No. TH-39/00-3).

[‡] The atomic coordinates have been deposited in the Protein Data Bank (PDB) under accession codes 1TZ4 ([hPP$^{19-23}$]-pNPY) and 1TZ5 ([pNPY$^{19-23}$]-hPP).

* Corresponding author. Address for correspondence: Institute of Organic Chemistry, University of Zurich, Winterthurerstrasse 190, CH-8057 Zurich, Switzerland. Phone: +41-1-635 42 63. Fax: +41-1-635 68 33. E-mail: oliver.zerbe@oci.unizh.ch.

[§] ETH Zurich.

[||] Present address: Department of Biochemistry and Biophysics, Stockholm University, Sweden. E-mail: mirjam@dbb.su.se.

[⊥] Monash University.

[#] Present address: Shionogi Research Laboratories, Shionogi & Co. Ltd. E-mail: hiroshi.kamimori@shionogi.co.jp.

[▽] E-mail: folkers@pharma.ethz.ch.

[○] E-mail: mibel.aguilar@med.monash.edu.au.

[◇] University of Leipzig. E-mail: beck-sickinger@uni-leipzig.de.

[¥] University of Zurich.

[1] Abbreviations: BH, Bolton−Hunter; CHAPS, 3-[(3-cholamidopropyl)dimethylammonio]propanesulfonic acid; DMPC, dimyristoylphosphatidylcholine; DMPG, dimyristoylphosphatidylglycerol; DPC, dodecylphosphocholine; doxyl, (4,4-dimethyl-3-oxazolidine-N-oxyl); HSQC, heteronuclear single-quantum correlation; $^3J_{HN\alpha}$, vicinal spin−spin coupling constant between the backbone H^N proton and the α-proton; K_{assoc}, association constant; NOE, nuclear Overhauser effect; NOESY, nuclear Overhauser enhancement spectroscopy; $^{15}N\{^1H\}$-NOE, nuclear Overhauser enhancement of ^{15}N saturation of ^1H; NPY, neuropeptide (h, human; p, porcine); PP, pancreatic polypeptide (a, avian; b, bovine; h, human); PYY, peptide YY (h, human; p, porcine); RMSD, root-mean-square deviation; RU, response units (arbitrary unit in SPR); SPR, surface plasmon resonance; TOCSY, transverse relaxation-optimized spectroscopy.

10.1021/bi0501232 CCC: $30.25
Published on Web 05/28/2005

Table 1: Sequences of Bovine PP, Human PP, Porcine NPY, NPY Chimera, and PP Chimera[a]

Peptide	Amino acid residue sequence
bPP	APLEP EYPGD NATPE QMAQY AAELR RYINML TRPR Y-NH_2
hPP	APLEP VYPGD NATPE QMAQY AADLR RYINML TRPR Y-NH_2
pNPY	YPSKP DNPGE DAPAE DLARY YSALR HYINLI TRQR Y-NH_2
[$pNPY^{19-23}$]-hPP	APLEP VYPGD NATPE QMA**RY YSA**LR RYINML TRPR Y-NH_2
[hPP^{19-23}]-pNPY	YPSKP DNPGE DAPAE DLA**QY AAD**LR HYINLI TRQR Y-NH_2

[a] Residues of NPY and PP conserved among different species are underlined. Segment 19−23 in the chimera is printed bold.

Table 2: IC_{50} Values (nM) of NPY, PP and Chimeras at the hY_1, hY_2, hY_4, and hY_5 Receptors[a]

peptide	Y_1	Y_2	Y_4	Y_5
pNPY	0.2[b]	0.08[b]		
hNPY	0.23[c]−0.81[d]	0.016[d]−0.04[c]	1.9[d]−5.8[c]	0.06[c]−0.19[d]
[hPP^{19-23}]-pNPY	14.6[c]	1.0[c]	>1000[c]	191[c]
hPP	48.9[d]−>1000[c]	>1000[d]−>2000 [c]	0.008[d]−0.04 [c]	7.25[d]−58 [c]
[$pNPY^{19-23}$]-hPP	3.93[d]−50[c]	19.3[d]−23[c]	0.0008[d]−0.5[c]	0.73[d]−1.5[c]

[a] K_i values were determined in ref *39*. [b] Reference *33*. Radiolabels used: Y_1,Y_2, [^{125}I]-BH-pNPY. [c] Reference *5*. Radiolabels used: Y_1,Y_2,Y_5, [^{3}H]-propionyl-NPY; Y_4, [^{125}I]-hPP. [d] Reference *39*. Radiolabels used: Y_1,Y_5, [^{125}I]-BH-pNPY; Y_2, [^{125}I]-h-PYY; Y_4, [^{125}I]-hPP.

It was soon hypothesised that the very different receptor subtype binding affinities may be encoded in certain parts of the amino acid sequence of the peptides. Therefore different PP/NPY chimeras were synthesized in order to combine biological features of both into a single peptide and their binding properties were characterized (*5*). Various single or multiple mutations were examined. Interestingly, swapping residues 19−23, part of the C-terminal α-helix, between NPY and PP led to interesting changes in binding affinities, whereby introducing the NPY segment into PP caused remarkably higher affinities at the Y_1 and Y_2 subtypes and to about 10−20-fold higher affinity at the Y_5 receptor without concomitant loss of binding affinity at the Y_4 receptor (Table 2). In addition, exchanges that caused an interesting modification in the binding properties were combined leading to the development of agonists with picomolar affinities at the Y_5 receptor. For an overview of these experiments see Cabrele et al. (*6*).

PP and NPY display characteristically different structures in solution. The first structure for a member of this family was the crystal structure of avian pancreatic polypeptide (aPP) (*7*). Therein, aPP displays an elongated shape and contains two regions of secondary structure. Residues 1−8 form an extended polyproline helix which is connected by a β-turn to a C-terminal α-helix comprising residues 14−31. This structural motif later became known as the PP-fold and was confirmed to also exist in solution by the NMR structure of bPP (*8*). PP and NPY share a sequence homology of about 50%, and the C-terminal half is characterized by an amphiphilic helix and therefore such a PP-fold was also postulated for NPY (*9*). Later structures however established that NPY forms dimers in solution in which the N termini remain flexible (*10*−*12*). Representative structures of the NMR ensembles of hNPY and bPP demonstrating the difference in back-folding are depicted in Figure 1.

In 1984 Kaiser and Kezdy recognized that only a few key residues of peptide hormones are involved in forming contacts to their receptors and proposed that composition and amphiphilicity of an α-helix might be important for

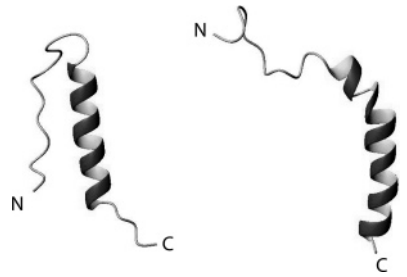

FIGURE 1: Schematic representation of the secondary structures of bPP (left) and pNPY (right) when unligated in solution as determined by Li et al. (*8*) and Monks et al. (*10*), respectively.

biological activity such that the helix promotes interactions with biological membranes (*13*). These ideas were later refined by Schwyzer et al. in his membrane compartment theory (*14*−*16*). The theory proposes that the membrane induces a conformation that is partially preformed for receptor binding and that it is the conformation of the membrane-bound species that is recognized by the receptor. Accordingly, we determined the structures of pNPY (*12*), [Ala^{31},Pro^{32}]-pNPY (*17*), bPP (*18*), and pPYY (*19*) when bound to phospholipid micelles and discovered significant differences from the solution structures.

Because the exchange of the helical segment 19−23 leads to dramatically altered receptor binding properties (Table 2), we decided to characterize the two chimeras [hPP^{19-23}]-pNPY and [$pNPY^{19-23}$]-hPP in solution and when bound to DPC micelles, as receptor binding data were available for these two peptides. Comparison of the structural data to those from the parental peptides should reveal whether structural changes occur that might explain the differences in receptor binding affinities. Of particular interest to us was whether these structural differences were larger in the presence or the absence of the phospholipid micelles. Special attention was given to potentially different back-folding propensities of the peptides in solution. Using surface plasmon resonance we have additionally determined whether the chimeric peptides display largely altered membrane association af-

finities. In particular we were interested to see whether and how these membrane-binding data are related to the trends observed for receptor binding affinities.

EXPERIMENTAL PROCEDURES

Cloning, Expression and Purification of Peptides. Following the strategy described by Kohno et al. (*20*) we expressed the peptides as N-terminally decahistidine-tagged yeast ubiquitin fusion-protein. The uniformly ^{15}N labeled peptides were grown on minimal media containing ^{15}N-NH_4Cl as sole nitrogen source. After enzymatic cleavage with the ubiquitin hydrolase (YUH), C-terminal amidation was performed by enzymatic conversion of an extra Gly residue into an amide function using the α-amidating peptidyl glycine amidase (PAM). We started with a plasmid containing the DNA coding for the parental peptides (*12*, *18*) and designed primers coding for the exchanged segments 19−23. In the case of [pNPY$^{19-23}$]-hPP the additional point mutation Glu6Val had to be introduced by site directed mutagenesis. The sequences were confirmed using dideoxy sequencing. Expression, isolation and purification were performed following the method of Kohno (*20*) as previously described (*18*). Purity was checked by HPLC on a RP_{18} column, and completeness of the amidation reaction was confirmed by electrospray ionization mass spectrometry (^{15}N-[hPP$^{19-23}$]-pNPY theoretical mass 4214.5 amu, experimental mass 4214.4 amu; ^{15}N-[pNPY$^{19-23}$]-hPP theoretical mass 4329.8 amu, experimental mass 4330.0 amu; SSQ710, Finnigan, San Jose, CA).

NMR Spectroscopy. The peptide concentration for structure elucidation was approximately 2.0 mM, 1.0 mM for the measurements of the $^{15}N\{^1H\}$-NOE and 0.4 mM for the spin-label experiments. For spin-label experiments and relaxation data uniformly ^{15}N labeled peptides were used. The peptides were dissolved in a solution containing 300 mM DPC micelles in 90% H_2O/10% ^2H_2O at pH 6.0 (uncorrected meter reading). For examination of the aliphatic region the samples were lyophilized and redissolved in 99.9% ^2H_2O. For the $^{15}N\{^1H\}$-NOE of unligated peptides, samples of uniformly ^{15}N labeled peptides were used at concentrations of approximately 1.0 mM, pH 3.1 or pH 4.6 for [hPP$^{19-23}$]-pNPY and [pNPY$^{19-23}$]-hPP, respectively. The temperature was set to 305 K for [hPP$^{19-23}$]-pNPY and 301 K for [pNPY$^{19-23}$]-hPP. Spectra for assignment and structure determination of the micelle-bound peptides were recorded at 310 K on a Bruker AVANCE 700 MHz spectrometer or a Bruker DRX-600 spectrometer, ^1H-NOE relayed [^{15}N,^1H]-HSQC and the $^{15}N\{^1H\}$-NOE spectra were measured on a DRX-500 spectrometer. [^1H,^1H]-clean TOCSY and zero-quantum suppressed NOESY experiments were performed as described previously (*12*). For further details of spectroscopy and data evaluation see Bader et al. (*12*). The micelle integrating spin-label 5-doxyl-stearic acid was used to determine the orientation of the peptides with respect to the membrane surface. The methodology was described in detail for pNPY (*12*).

Structure Calculation. Sequential resonance assignment was performed largely following the procedures developed by Wüthrich and described in more detail in Bader et al. (*12*). Differences in chemical shifts with respect to those of the parental peptides were small for parts of the molecules not containing mutations. The complete list of assignments of ^1H and ^{15}N chemical shifts of the two chimeras bound to DPC micelles as well as the assignment of their [^{15}N,^1H] correlation map in solution is provided in the Supporting Information.

The structure calculations were done by restrained molecular dynamics in dihedral angle space using the standard simulated annealing protocol as implemented in the program DYANA (*21*). The distance restraints were obtained from NOESY spectra recorded with a mixing time of 75 ms measured either in 90% H_2O/10% ^2H_2O or in 99.9% ^2H_2O. $^3J_{HN\alpha}$ coupling constants <6.0 Hz indicate the presence of an α-helix and were included in the structure calculations. Such reduced scalar couplings were observed for residues Ala^{12}, Ala^{14}, Leu^{17}−Leu^{30}, Arg^{33}, and Gln^{34} in [hPP$^{19-23}$]-pNPY and for residues Thr^{13}, Met^{17}−Asn^{29}, Leu^{31}, and Arg^{33} in [pNPY$^{19-23}$]-hPP. The Supporting Information includes a graphical overview of the applied restraints and a table containing the $^3J_{HN\alpha}$ coupling constants. The 20 refined structures with lowest energy contributions from intramolecular interactions were chosen to represent the NMR ensemble. The quality of the final structures was assessed using the program PROCHECK-NMR (*22*). Further analysis of the conformers including calculation of root-mean-square deviations (RMSDs) was performed in the molecular graphics program MOLMOL (*23*), which was also used to prepare all figures. The determined structures have been deposited in the Research Collaboratory for Structural Bioinformatics protein database under accession codes 1TZ4 ([hPP$^{19-23}$]-pNPY) and 1TZ5 ([pNPY$^{19-23}$]-hPP).

Surface Plasmon Resonance (SPR) Experiments. Small unilamellar vesicles (SUVs) (50 nM) were prepared in 20 mM phosphate buffer (pH 6.8) containing 150 mM sodium chloride using procedures described by us in detail previously (*24*). The pH for the SPR measurements was chosen to best mimic biological conditions while still providing sufficient solubility of the peptides. Unfortunately, rapid hydrogen exchange hampers NMR spectroscopy and hence a slightly more acidic pH was required for these experiments. The L1 sensor chip was installed in a BIACORE 3000 analytical system (Biacore, Uppsala, Sweden), and the surface was washed by injecting 5 μL of 20 mM CHAPS at a flow rate of 5 μL/min. SUVs (80 μL) were immediately applied to the sensor chip surface at a flow rate of 2 μL/min. Multilamellar structures were removed from the lipid surface by injecting 30 μL of 10 mM sodium hydroxide at a flow rate of 50 μL/min, resulting in a stable baseline. Peptide solutions (50 μL) in the concentration range between 2.5 and 25 μM (20 mM phosphate buffer, pH 6.8) were injected during 200 s at a flow rate of 15 μL/min at 25 °C. Upon completion of injection, buffer flow was continued for 600 s to allow for complete dissociation. The affinity of each peptide for the lipid surface was determined from analysis of a series of response curves collected at seven different peptide concentrations.

The sensorgrams for each peptide−lipid interaction were analyzed by curve fitting using numerical integration analysis. Kinetic data were extracted by simultaneously fitting the peptide sensorgrams obtained at seven different concentrations using BIA evaluation software (version 4.1). A two-state model, describing association followed by a conformational or orientational change—in our case triggered by membrane insertion—was applied to the resultant peptide binding curves to estimate the association and dissociation

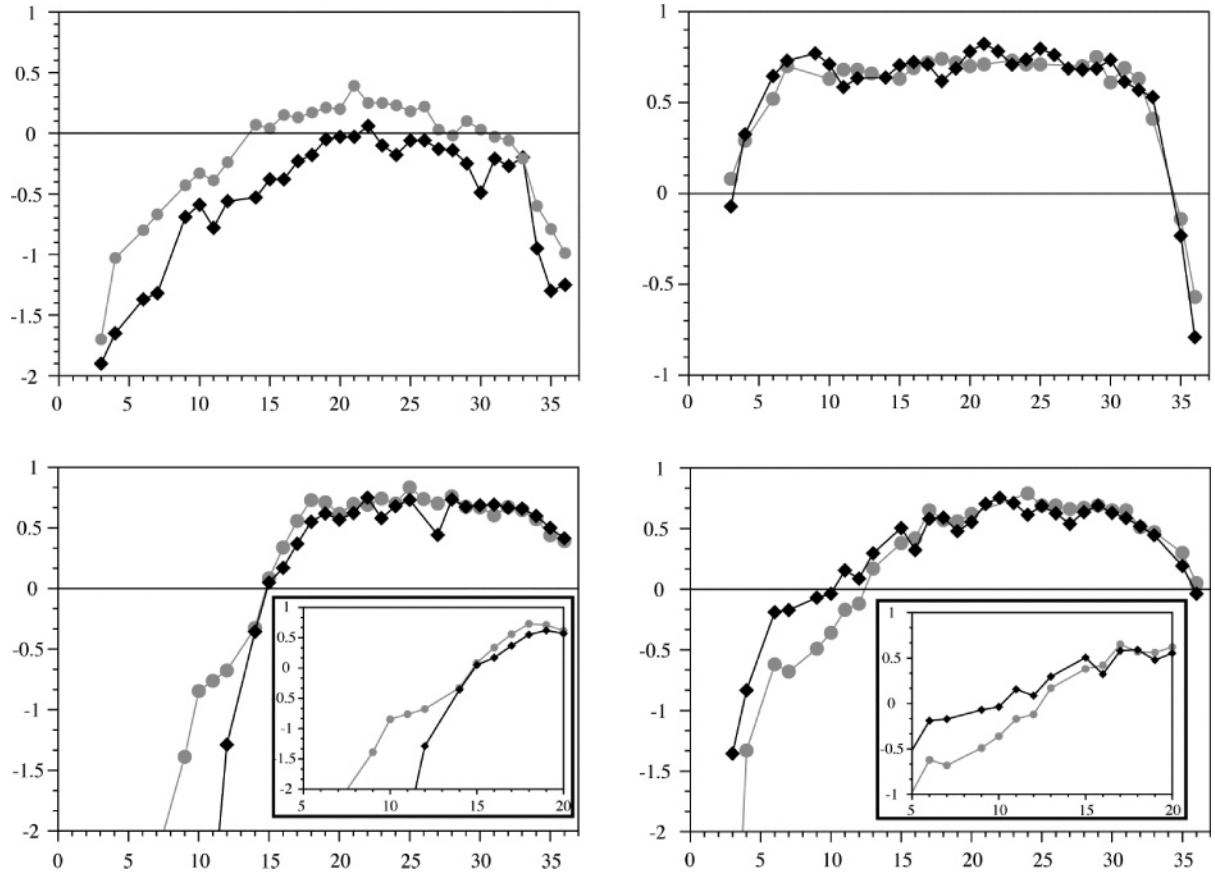

FIGURE 2: Values for the $^{15}N\{^1H\}$-NOE unligated in solution (top) and when bound to DPC micelles (bottom) vs sequence. Left: Data for [hPP$^{19-23}$]-pNPY (black) and NPY (gray). Right: Data for [pNPY$^{19-23}$]-hPP (black) and PP (gray). Data for residues 5−20 of the micelle-bound forms are displayed on an expanded scale for clarity in the corresponding insets.

rate constants. The corresponding differential rate equations for this reaction model are represented by

$$dR_1/dt = k_{a1}C_A(R_{max} - R_1 - R_2) - k_{d1}R_1 - k_{a2}R_1 + k_{d2}R_2$$

$$dR_2/dt = k_{a2}R_1 - k_{d2}R_2$$

$$K_{assoc} = K_{assoc1}K_{assoc2} = (k_{a1}/k_{d1})(1 + k_{a2}/k_{d2})$$

in which k_{a1} or k_{a2} and k_{d1} or k_{d2} are the separate association and dissociation constants of the two processes occurring during binding and R_1 and R_2 the corresponding rate constants (*25*).

RESULTS

The Fold of the Peptides in Solution. A prominent feature of the solution structure of bovine PP is the occurrence of the so-called PP-fold, in which the otherwise largely unstructured N-terminal half of the molecule is back-folded onto the C-terminal α-helix. We showed recently by a careful comparison of structural data of a number of peptides from the NPY family with the corresponding $^{15}N\{^1H\}$-NOE data that the latter is an ideal parameter to quantify the extent of back-folding (*18*, *19*). We would like to emphasize here that the $^{15}N\{^1H\}$-NOE does not provide sufficient information to create secondary structure in general, but in our specific case, where the type of secondary structure to be expected is clear (and supported by a larger number of structures we determined the usual way), it is a reliable and fast method to define the length of the C-terminal helix and the extent of back-folding. In a rigid part of the molecule the $^{15}N\{^1H\}$-NOE will be close to 0.8 and exhibit smaller or even negative values for more flexible regions such as amide moieties of a freely diffusing N-terminal segment.

The values for the $^{15}N\{^1H\}$-NOE in aqueous solution are depicted in Figure 2. The differences between [hPP$^{19-23}$]-pNPY or pNPY (left) and [pNPY$^{19-23}$]-hPP or bPP (right) are much more pronounced than the differences between the chimeric and their parental peptides. The data for [hPP$^{19-23}$]-pNPY and pNPY display only few positive values with those from [hPP$^{19-23}$]-pNPY being lower than those of pNPY in the helical segment. Moreover, the NOE data indicate that the extent to which [hPP$^{19-23}$]-pNPY is folded is so low that it is very unlikely that the structure could be determined properly, provided that the peptide is structured at all. In the case of pNPY both the NMR structure and the $^{15}N\{^1H\}$-NOE data are incompatible with back-folding of the N terminus and, as [hPP$^{19-23}$]-pNPY displays even higher flexibility in the N-terminal region, back-folding can be safely excluded for both peptides.

The data for bPP and [pNPY$^{19-23}$]-hPP are virtually indistinguishable and clearly document rigidly back-folded peptides as described for bPP (*8*, *18*). The differences of corresponding values for bPP and [pNPY$^{19-23}$]-hPP are generally smaller than the error margins for determining those values.

Taking into account the high flexibility of [hPP$^{19-23}$]-pNPY we decided to not further structurally characterize the

Table 3:

peptide	lipid	rate constants (two-state reaction model) (2.5−25 μM) k_{a1} (1/(M s))	k_{d1} (1/s)	k_{a2} (1/s)	k_{d2} (1/s)	K_{assoc} (1/M)	$\chi 2$
bPP	PC	1340	6.54×10^{-2}	3.64×10^{-3}	2.92×10^{-3}	4.58×10^{4}	6.8
	PC/PG[a]	971	4.01×10^{-2}	4.43×10^{-3}	5.91×10^{-3}	4.23×10^{4}	7.2
pPYY	PC	472	3.00×10^{-2}	4.12×10^{-3}	1.71×10^{-3}	5.36×10^{4}	18
	PC/PG[a]	180	1.82×10^{-2}	3.41×10^{-3}	2.04×10^{-3}	2.63×10^{4}	45
pNPY	PC	501	1.74×10^{-2}	2.48×10^{-3}	1.81×10^{-3}	6.83×10^{4}	1200
	PC/PG[a]	385	4.78×10^{-2}	1.32×10^{-3}	2.57×10^{-3}	1.22×10^{4}	1900
[pNPY$^{19-23}$]-hPP	PC	12400	15.0×10^{-2}	1.21×10^{-3}	1.97×10^{-3}	5.09×10^{4}	3490
	PC/PG[a]	7270	11.1×10^{-2}	1.28×10^{-3}	2.20×10^{-3}	3.82×10^{4}	3830
[hPP$^{19-23}$]-pNPY	PC	427	13.5×10^{-2}	5.28×10^{-3}	1.21×10^{-3}	1.70×10^{4}	1.9
	PC/PG[a]	220	6.11×10^{-2}	5.56×10^{-3}	0.821×10^{-3}	2.79×10^{4}	3.1

[a] PC/PG (4:1, w/w).

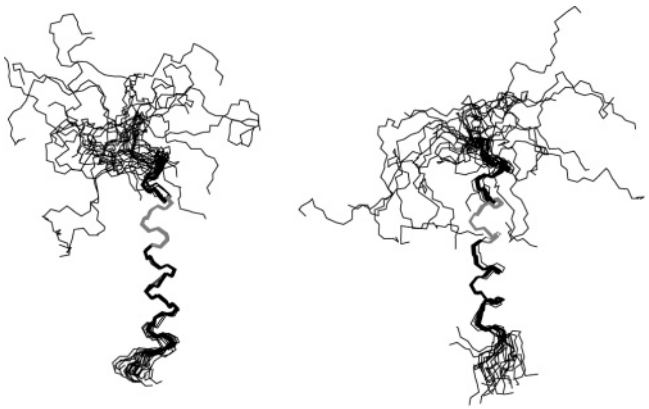

FIGURE 3: Superposition of the NMR ensemble of the 20 lowest energy structures of [hPP$^{19-23}$]-pNPY (left) and [pNPY$^{19-23}$]-hPP (right) with backbone atoms of residues 19−23 highlighted in gray.

chimeric peptides in the absence of a membrane model but limit our investigations to the prove that changes in back-folding propensities were not introduced by the mutations.

Properties of Micelle-Bound Peptides. Structures. As mentioned before, the $^{15}N\{^1H\}$-NOE gives information on the internal backbone dynamics of a peptide. The values for the four peptides bound to DPC micelles are presented in Figure 2. In general all peptides are segregated into a well-folded and into a flexible part. At the N terminus the negative values indicate flexibility, whereas in the α-helical segment in the C-terminal part positive values are observed confirming a rigid structure.

The raw NMR data as presented by the proton−proton NOEs and the $^3J_{HN\alpha}$ indicate overall similarity of pNPY and [hPP$^{19-23}$]-pNPY with subtle changes occurring at the N-terminal part of the α-helix (see Supporting Information). Although all α,*β* *i*,*i*+3 NOEs are found in both peptides for $i = 15$ to 18, pNPY additionally displays a NOE between Hα12 and H*β*15. The $^3J_{HN\alpha}$ scalar couplings display slightly larger values for [hPP$^{19-23}$]-pNPY when compared to pNPY, in particular in the segment 14−16, for which they are below 6 Hz for pNPY in contrast to the chimeras. The differences in the values of the $^{15}N\{^1H\}$-NOE are only minor; they nevertheless add further evidence to the view that the helix of the chimera in its N-terminal part is not as stable as in the parent peptide.

The energy-minimized conformers of [hPP$^{19-23}$]-pNPY were α-helical between residues Leu^{17} and Thr^{32}. In most of the structures $H^N_{i+4} \rightarrow CO_i$ hydrogen bonds are present in the segment between Asp^{16} and Thr^{32}, with the exception of Ala^{18}−Ala^{22}, which is probably caused by severe peak overlap for protons of the two residues thereby reducing the number of available restrains. In the α-helical segment Leu^{17}−Thr^{32} the RMSD is 0.42 (±0.18) Å for the backbone heavy atoms. [hPP$^{19-23}$]-pNPY has $^{15}N\{^1H\}$-NOE values similar to those of pNPY, which at the C terminus only a slightly decrease, supporting the view that the helical structure extends up to Tyr^{36}.

Table 4: RMSD Values (Å), Calculated for the Range Indicated[a]

peptide	14−31/32[b] backbone	14−31/32[b] heavy atoms	17−31/32[c] backbone	17−31/32[c] heavy atoms
pNPY	0.53 ± 0.20	1.51 ± 0.13	0.36 ± 0.17	1.49 ± 0.39
[hPP$^{19-23}$]-pNPY	0.77 ± 0.23	1.38 ± 0.20	0.42 ± 0.18	1.08 ± 0.27
bPP	0.53 ± 0.22	1.35 ± 0.34	0.31 ± 0.14	1.19 ± 0.28
[pNPY$^{19-23}$]-hPP	0.41 ± 0.20	1.55 ± 0.30	0.30 ± 0.20	1.55 ± 0.32

[a] A mean structure was used as a reference. [b] For pNPY and [hPP$^{19-23}$]-pNPY, the RMSD was calculated for residues 14−32; for bPP and [pNPY$^{19-23}$]-hPP, the RMSD was calculated for residues 14−31. [c] For pNPY and [hPP$^{19-23}$]-pNPY, the RMSD was calculated for residues 17−32; for bPP and [pNPY$^{19-23}$]-hPP, the RMSD was calculated for residues 17−31.

The superposition of the NMR ensemble of [hPP$^{19-23}$]-pNPY is displayed in Figure 3. Upon comparing pNPY and [hPP$^{19-23}$]-pNPY the most important difference observed in the computed structures is that in pNPY the helix starts at Ala^{14}, whereas Leu^{17} presents the first helical residue in the chimera. The different starting positions for the helix are well supported by differences in observed hydrogen bond patterns, as pNPY displays an additional $H^N_{i+4} \rightarrow CO_i$ hydrogen bond between residues 14−18. In the region 17−32, which is α-helical in all structures of both peptides, the RMSDs for the backbone atoms are of comparable magnitude. In pNPY regular $H^N_{i+4} \rightarrow CO_i$ hydrogen bonds occur up to Tyr^{36}, but only up to Thr^{32} in [hPP$^{19-23}$]-pNPY, for which an additional $H^N_{i+3} \rightarrow CO_i$ hydrogen bond is found between residues 31 and 34. The latter indicates a more 3_{10} helical character toward the C terminus, but the $^{15}N\{^1H\}$-NOEs (see Figure 2) and RMSDs (see Table 4) reveal no evidence for higher flexibility in this part.

Comparing [pNPY$^{19-23}$]-hPP and bPP, again subtle differences are observed in the raw NMR data of residues of the N-terminal segment of the α-helix. All α,*β* *i*,*i*+3 NOEs are found in both peptides for $i = 15$ to 18. In [pNPY$^{19-23}$]-hPP additional medium range NOEs between the *β*-protons of residue 12 or Hα of residue 13 and the *β*- or *γ*-protons of residues 16 and 17 are found (the latter is *very* weak in bPP).

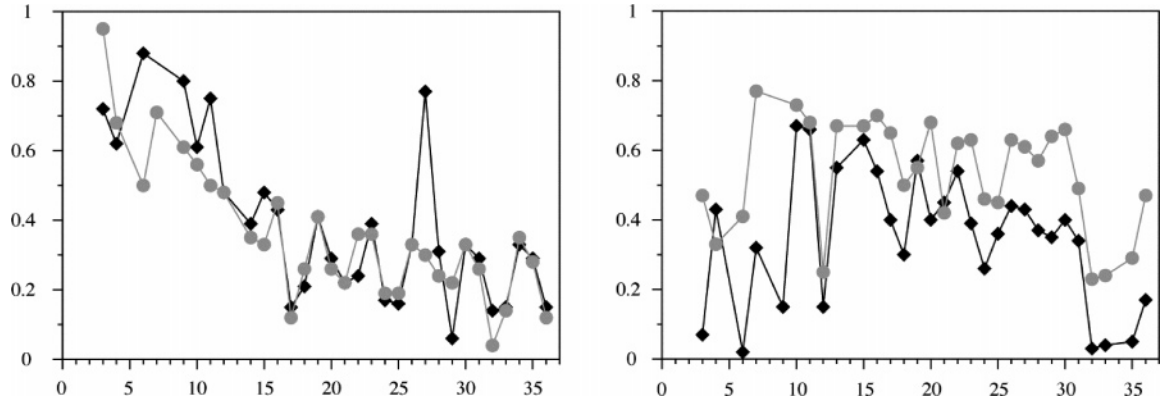

FIGURE 4: Relative signal intensities in [^{15}N,^{1}H]-HSQC spectra of micelle associated peptides in the presence of the spin-label 5-doxyl-stearic acid with respect to a reference spectrum recorded in the absence of spin-label. Left: [hPP$^{19-23}$]-pNPY (black) and NPY (gray). Right: [pNPY$^{19-23}$]-hPP (black) and PP (gray).

For residues 16 to 18 the $^{3}J_{HN\alpha}$ couplings are smaller. Similarly to the situation in NPY/[hPP$^{19-23}$]-pNPY scalar couplings in the segment 12−13 are unchanged. Furthermore, we measured higher ^{15}N{^{1}H}-NOEs for [pNPY$^{19-23}$]-hPP in that segment (see inset in Figure 2).

Examination of the energy-minimized structures of [pNPY$^{19-23}$]-hPP revealed an α-helix between Met^{17} and Leu^{31} in all structures (see Figure 3 for a superposition of the NMR ensemble). However, in most of the conformers the helix already begins at Pro^{14}. The $H^{N}_{i+4} \rightarrow CO_i$ hydrogen bonds are present in almost all of the structures in the segment from Gln^{16} to Thr^{32}. Additional hydrogen bonds are found between Thr^{13}−Met^{17} and Pro^{14}−Ala^{18}. At the N and C termini of the helix $H^{N}_{i+3} \rightarrow CO_i$ hydrogen bonds exist, too. Best convergence of the resulting structures was observed for the region 17−31 with RMSD values of 0.30 (±0.19) Å for the backbone heavy atoms, and only slightly increases upon including residues 14−31 to a value of 0.41 (±0.20) Å (see also Table 4). We conclude that the helix starts at Pro^{14} and is longer when compared to the parental peptide bPP. We like to emphasize here that the extension of the helix is well reflected in higher values for the heteronuclear NOE (see inset in Figure 2).

The structure comparison of bPP and [pNPY$^{19-23}$]-hPP reveals high similarity for the helical segment. However as mentioned above, the α-helix is N-terminally extended in [pNPY$^{19-23}$]-hPP. In 14 out of 20 structures the helix in [pNPY$^{19-23}$]-hPP already starts at residue 14, whereas for bPP this extended helix is an exception. This difference is also reflected in the weaker increase in RMSD values upon including residues 14−16 for [pNPY$^{19-23}$]-hPP compared to PP. Otherwise, bPP and [pNPY$^{19-23}$]-hPP are very similar in the helical segment encompassing residues 17 to 31 with backbone RMSDs of 0.31 (±0.14) Å for PP and 0.30 (±0.19) Å for the chimera. Another obvious difference is the fact that the helical fold extends further to the C terminus in [pNPY$^{19-23}$]-hPP with the consequence that the termini seem to point into different directions. We more closely investigated this apparent difference and noticed that the H^{N} shifts of residues 30 and 33 are highly overlapped in bPP but not in the chimeric peptide. Due to this overlap a number of *i*,*i*+3 restraints sampled in the case of the chimera are absent in bPP so that the last helical turn is missing in bPP. We therefore believe that this difference is an artifact due to a lack of restraints in bPP in that particular part. Again, we like to emphasize the importance of the ^{15}N{^{1}H}-NOE (Figure 2), which up to Arg^{33} assumes very similar values in the two peptides. Nevertheless, it is perfectly clear that the terminal tripeptide is much more rigid in pNPY or [hPP$^{19-23}$]-pNPY when compared to bPP or [pNPY$^{19-23}$]-hPP, both of which contain Pro at position 34.

Orientation on the Membrane. To probe the spatial orientation of the peptides on the micelle surface we conducted spin-label experiments as previously described by us (*12*). Figure 4 shows the relative residual signal intensities of the two chimeric and their parental peptides vs the sequence recorded in [^{15}N,^{1}H]-HSQC spectra with/without spin-label. The data of [hPP$^{19-23}$]-pNPY are qualitatively similar to those of NPY with the exception of remarkably high remaining signal intensity (0.77) of Tyr^{27}, which leads also to an extraordinarily large difference in residual signal intensities between Tyr^{27} and Asn^{29}. We examined the spectra carefully but could safely exclude resonance overlap or misassignment. Similarly to the situation encountered for pNPY, no attenuation in signal intensity for residues at the N terminus could be observed. Residues Leu^{17}, Ala^{21}, Leu^{24}, Arg^{25},Asn^{29}, Thr^{32}, Arg^{33}, and Tyr^{36} were affected to the largest extent in [hPP$^{19-23}$]-pNPY. As expected, these are mainly hydrophobic or Arg residues, the latter being frequently found at the membrane water interface (*26*).

[pNPY$^{19-23}$]-hPP exhibited values qualitatively very similar to those of bPP, however, [pNPY$^{19-23}$]-hPP in general shows stronger attenuation of signal intensities than bPP. We attribute the absolute differences largely to the fact that [pNPY$^{19-23}$]-hPP binds more tightly to the DPC micelle, a view that is supported by the SPR data (vide infra). For both peptides, interactions between residues of the N terminus and the micelle interface were found, in clear contrast to the situation for pNPY or its chimera. Interestingly, a slight shift in the orientation can be observed in the helical segments: residues Ala^{18}, Ala^{21}, and Arg^{25} showed strongest effects upon spin-label addition in bPP vs Ala^{18}, Tyr^{20}, and Leu^{24} in the case of the chimeric peptide. In both peptides the largest effects are seen for the C-terminal residues Thr^{32}, Arg^{33}, and Arg^{35}. Moreover, hPP has a Val^{6}, whereas in bPP a Glu is found at this position, which probably largely accounts for the stronger reductions in the N-terminal residues. As described in more detail for bPP and pNPY (*12*, *19*) we measured H/^{2}H exchange for both chimeras. In general the data were similar to those of their parental

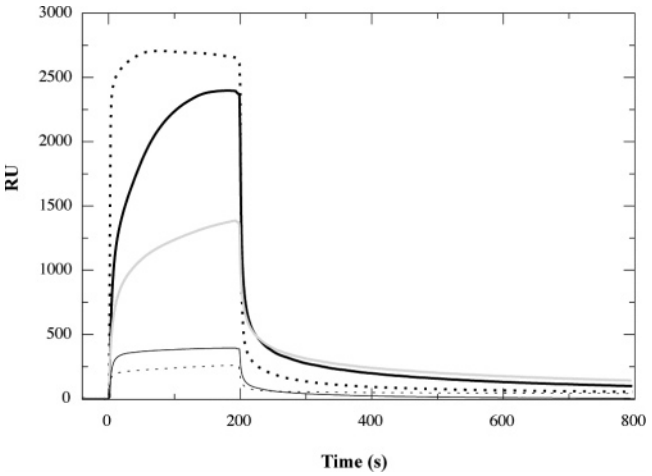

FIGURE 5: Representative surface plasmon (BiaCore) sensorgrams of 25 μM solutions of NPY (solid thick line), PP (solid thin line), PYY (gray line), [pNPY19−23]-hPP (dotted thin line), and [hPP19−23]-pNPY(dotted thick line), pH = 6.8, 20 mM phosphate buffer, 25 °C on DMPC-coated surfaces.

peptides with the exception that for [pNPY$^{19-23}$]-hPP even after 3 days the amide protons of residues Leu^{24}, Tyr^{27}, and Ile^{28} could still be detected, whereas for all other peptides after 1 h only weak peaks were observable (data not shown).

Membrane-Binding Affinities. In case receptor binding is preceded by membrane binding large changes in the latter are expected to translate into significant changes for receptor binding. We have therefore used surface plasmon resonance (SPR) spectroscopy to determine the kinetic data for membrane association of the peptides at pH 6.8 in 20 mM phosphate buffer. SPR spectroscopy enables the real-time measurement of binding of the peptides to biomimetic surfaces and thereby facilitates extraction of the kinetic data for membrane association. In our studies we have coated the vesicle capture (L1) chip (a dextran matrix modified by lipophilic compounds) with DMPC or a 4:1 w/w mixture of DMPC/DMPG vesicles, with the latter mimicking partially negatively charged membranes (*25*). Table 3 presents the kinetic data as derived from the SPR measurements, and representative sensorgrams are depicted in Figure 5. The values for χ^2 are very low for bPP, pPYY, and [hPP$^{19-23}$]-pNPY, indicating good fits of simulated curves to the experimental data. Poorer fits were obtained for pNPY and [pNPY$^{19-23}$]-hPP, which is partially due to the higher RU values but may also reflect a more complex binding mechanism for these peptides, and hence data have to be used more cautiously.

As a result of our measurements we notice that the overall association rates are *moderate* and the spanned range of association constants is rather small. Surprisingly, binding to the zwitterionic bilayers is generally tighter than to the negatively charged bilayers except for [hPP$^{19-23}$]-pNPY.

DISCUSSION

We have taken a structural approach to investigate whether for hormones of the NPY family membrane association precedes receptor binding as proposed by the membrane compartment theory (vide supra) (*14*, *15*). Herein, we compare structures and internal backbone dynamics of pairs of peptides both in solution and when bound to the membrane mimicking phospholipid micelles. Structural features in both environments are related to biological data in order to investigate which of them better agree with the relative affinities at the various Y receptors.

Recently, we have shown that pNPY and pPYY, a pair of peptides with highly similar binding affinities at all Y receptors, display very different structures in solution but an almost identical fold in the micelle-bound state, indicating that it is the membrane-bound state that is recognized by the receptors (*19*). Herein, we investigate a pair of peptides with rather different binding properties at the receptor subtypes and find significant structural differences only in the micelle-bound state.

NPY and PP have very different pharmacological profiles and structural features. The chimeric peptides demonstrate that by swapping as few as five residues between the two peptides the pharmacological properties can be dramatically altered. Because of the large differences in biological activities between the parent peptides and the chimeras and considering the fact that PP is back-folded and NPY not, we initially speculated that the changes in affinities were caused by changes in back-folding propensities introduced by swapping the segment 19−23. From the similarity in their ^{15}N{^{1}H}-NOE values it is evident that bPP and [pNPY$^{19-23}$]-hPP are both perfectly back-folded. In contrast, pNPY clearly displays no PP-fold in solution. The ^{15}N{^{1}H}-NOE data reveal that [hPP$^{19-23}$]-pNPY is even more flexible than pNPY. Our data, therefore, clearly show that chimeras and parent peptides possess identical back-folding propensities, when unligated in solution, and hence this feature is unlikely to account for the observed differences.

To summarize the structural investigation of the micelle-bound states [hPP$^{19-23}$]-pNPY is much more similar to its parental peptide pNPY than to bPP and for [pNPY$^{19-23}$]-hPP we encounter a very similar situation. Structural differences between pNPY or [hPP$^{19-23}$]-pNPY and [pNPY$^{19-23}$]-hPP or bPP largely account for differences in the C-terminal conformation, which are most likely due to the presence of Pro^{34} in the latter two. The most noticeable result of swapping the segments comprising residues 19 to 23 between pNPY and bPP (^{19}RYYS^{23}A in NPY vs ^{19}-QYAA^{23}E in hPP) is the N-terminal extension of the helix in the case of [pNPY$^{19-23}$]-hPP, respectively the truncation in [hPP$^{19-23}$]-pNPY with respect to their parental peptides. We would like to add here that exact structures of shorter peptides, which lack a well-defined core and in which the proton density of side-chain protons is low, still present a problem and we have therefore extensively used the ^{15}N-{^{1}H}-NOE to verify that the differences in the computed structures are real and do not present artifacts of the structure calculation. We have noticed when comparing pNPY with [pNPY$^{19-23}$]-hPP that the former displays medium-range NOEs between protons of residues 12 and 15 whereas in the case of the latter NOEs between residues 12 and 16 or 17 are observed. In addition, these medium-range NOEs are absent ([hPP$^{19-23}$]-pNPY) or very weak (bPP) for those peptides in which the helices are shorter and which also display lower membrane binding affinities. All data such as scalar couplings or values of the heteronuclear NOE indicate that the segment around residues 12 to 14 is not rigidly structured. However, the NOEs between residues 12 and 15 observed for NPY are compatible with a *transient linear* extension of the α-helix. In contrast, the NOEs between

Hα12 and protons from residues 16 and 17 in [pNPY$^{19-23}$]-hPP indicate that the *turn* present in the solution structure of PP, which leads to the back-fold, also exist *transiently* in the micelle-bound state. But it is also clear that in the membrane-mimicking environment no contacts between protons of residues 3−8 and protons from the C-terminal helix are found and hence a significant extent of back-folding can be excluded. Moreover, we did not observe medium-range NOEs in any of the investigated peptides in the segment comprising residues 1 to 12 indicating that no residual structure exists in that part of the peptide.

The reasons for the observed structural changes in the C-terminal α-helix are not absolutely clear yet. We notice that by exchanging Arg^{19} by Gln^{19} and Ala^{23} by Glu^{23} the charge in that segment is reversed. Interestingly, membrane binding generally becomes tighter once positive charges are increased, as demonstrated by biophysical methods for many membrane-active peptides (*24*, *25*), and our SPR data recorded on the DMPC surface indicate this also to be valid in our case (vide infra). Increasing membrane-binding affinities may then via the coupled partitioning−folding mechanism (*27*) lead to a better-stabilized secondary structure in that segment. On the contrary, negatively charged residues like Glu have particularly unfavorable membrane partitioning properties; therefore this segment is less stabilized by membrane binding. Of course, different helix-forming propensities of the residues, e.g. the much higher propensity of Arg (*28*), may also contribute to the difference in helix stability observed in that part. Recently, replacement of a Glu residue in the parathyroid hormone (PTH) by Arg was reported to result in a similar helix-stabilizing effect, propagating N-terminally from the place of the mutation (*29*).

Orientation on the Membrane and Membrane-Binding Affinity. Spin-label data of pNPY and [hPP$^{19-23}$]-pNPY (Figure 4, left) indicate that the membrane interface is highly similar, and only differences for Tyr^{27} and Asn^{29} are substantial, the reason for this difference being not clear yet. His is found at position 26 in both [hPP$^{19-23}$]-pNPY and pNPY, a residue for which p*K* values in the range between 4.9 and 6.6 in the presence of DPC micelles have been measured previously (*30*). A possible explanation is that the protonation state might have changed from His^0 in NPY to His$^+$ in the chimera, resulting in diminished anchoring of that residue in the interface (*31*). Signal attenuations for [pNPY$^{19-23}$]-hPP are generally stronger than for bPP (Figure 4, right). Regardless of this point the micelle-binding topology is highly similar for bPP and [pNPY$^{19-23}$]-hPP in the C-terminal pentapeptide, which is believed to be important for receptor activation. The difference in the N-terminal part of the molecules is most likely due to the additional Glu6Val point mutation. This view is supported by the fact that we measured much less reduction in that segment for a mutant of bPP, in which the strong membrane anchor Tyr^7 has been replaced by Ala (data not shown). This additional membrane anchor may in principle also account for the obvious changes in rigidity as reflected in the heteronuclear NOE in the N-terminal segment. Since we also observe these changes between NPY and its chimera, for which no difference in sequence of the N-terminal segment exists, we rather attribute these (small) effects to the conformational changes at the N cap of the helix.

The data for overall membrane-binding affinities as derived from our SPR measurements follow the expected trend on the neutral (zwitterionic) membranes. The overall association constants are correlated to the overall charge in the C-terminal helix: For [pNPY$^{19-23}$]-hPP binding is slightly improved (Glu^{23} → Arg^{19} exchange), whereas it is reduced for [hPP$^{19-23}$]-pNPY (Arg^{19} → Glu^{23} exchange). Even more importantly, partitioning of Arg residues into the membrane water interface is less unfavorable for Arg (0.81 kcal mol^{-1}) when compared to Glu (2.2 kcal mol^{-1}) (*32*). Additionally, a Tyr residue is introduced at position 21 in [pNPY$^{19-23}$]-hPP, a residue frequently found in the interfacial region of membranes (*26*). The trends in behavior for binding to negatively charged membranes are more complicated and difficult to understand. However, the differences between wild-type peptides and chimeras are much less pronounced.

To conclude, differences in peptide−membrane interactions are largely due to changes in membrane affinity but not in membrane-binding topology.

Structure−Activity Relationships. Extensive replacement studies combined with testing of receptor binding have been performed for hNPY (*33*), but much fewer data are available for PP (*34*, *35*). With respect to the receptors, Walker et al. have proposed that acidic residues on the extracellular loops are involved in binding (*36*). For the peptides from the NPY family two features were believed to be important: First, it could be shown in the case of hNPY that the two C-terminal arginines at positions 33 and 35 are essential for receptor activation (*33*, *37*). It is likely that they interact with the acidic receptor residues found essential for receptor activation. Second, the extraordinarily stable PP-fold, observed in the crystal (*7*) and solution structure (*8*) of PP, was believed to be an important feature for all members of this family. However it could be shown later that NPY (*10*, *12*, *38*) does not share this structural feature in solution.

Although not all peptides adopt this PP-fold in solution, it could be of importance in the case of PP and PYY. In our work we therefore attribute much attention to the question whether the peptides are back-folded in solution and to the conformation of the C-terminal pentapeptide, which is most probably directly involved in receptor-binding. As NPY and PP display large differences in receptor subtype binding profiles, the question emerged whether these differences are due to the propensities of the molecules to adopt the PP-fold. Although we have not explicitly solved the structures of the two chimeric peptides in solution, the ^{15}N{^{1}H}-NOE data unambiguously prove that the large changes in binding affinity profiles observed for the chimeric peptides are *not* accompanied by changes in their propensity to adopt the PP-fold in solution. Therefore, changed propensities to adopt the PP-fold in solution cannot account for the observed differences in pharmacology.

The introduction of the PP segment 19−23 into NPY leads to a decrease in binding affinity at all Y receptor subtypes. Surprisingly, the loss is even strongest for the Y_4 and Y_5 receptors, exactly those receptors that are activated by PP. This already indicates that features responsible for the (sub)-nanomolar affinities of NPY toward the Y_1, Y_2, and Y_5 subtypes and of PP toward Y_4 are not maintained in [hPP$^{19-23}$]-pNPY. The most prominent alteration upon introduction of the pNPY segment 19−23 into hPP is a remarkable affinity increase at the Y_1 and Y_2 receptors

indicating that some of the binding potency of NPY for the Y_1 and Y_2 receptor is introduced into [pNPY$^{19-23}$]-hPP. At the receptor subtypes originally being targeted by PP the changes are much smaller (see Table 2). The main structural difference is the extension of the α-helix toward the N terminus. Whether this change is due to better anchoring of the N terminus of the helix onto the membrane or due to higher helix propensity caused by the introduction of an Arg residue (or both) remains unclear. Interestingly, the single point mutant [Arg^{19}]-hPP shows similar binding profiles at the Y_1 and Y_5 receptors but stronger binding at the Y_4 receptor when compared to [pNPY$^{19-23}$]-hPP (Y_2 not tested (*5*); exact data: unpublished results) so that we attribute most of the changes, at least at the Y_1 and Y_5 receptors, to the introduction of this cationic residue.

CONCLUSIONS

With the present knowledge it is not possible to decide whether a structural difference, namely, the extension/truncation of the helix and/or particular side-chain interactions, is responsible for the encountered altered receptor-binding properties. The latter may also lead to altered binding affinities to the membranes. Our SPR data for neutral membranes do indeed indicate that the change in charge in that segment leads to noticeable differences for membrane-binding affinities. However, the binding affinities toward the membranes are *moderate* only, and it is unlikely that the differences account for the observed dramatic differences in binding at the various receptor subtypes. The membrane binding constant K_{assoc} describes a dynamic equilibrium between peptides free in solution and when bound to the membrane. If this constant is sufficiently high, a significant part of molecules will be associated with the membrane and rebinding will occur quickly. Our preliminary data indicate that peptides from the NPY family retain their membrane-induced conformation when they dissociate from the membrane, provided they remain in the vicinity, where the solvent properties (e.g. the dielectric constant) have not changed dramatically (data not shown). Importantly, moderate binding affinities would allow the peptides to come off the membrane in order to diffuse into the receptor binding pockets while still providing enough affinity to the membrane to guide them toward the receptors and to facilitate their recognition.

We have recently proposed that electrostatics, the importance of which of course depends on the exact positioning of the peptides with respect to the membrane−water interface, may play a more prominent role for recognition of these peptides by their G protein coupled receptors when compared to protein−protein (or protein−ligand) interactions in bulk solution (*18*). In all presently known NPY sequences a single *cationic* residue is found in the segment 19−23, and the same is true for all sequences of the peptide YY (PYY), which displays biological data similar to those of NPY. In contrast, almost all PP sequences contain a single *anionic* residue in that part of the molecule. We have also noticed that some of the extracellular loops of the Y receptors are quite different in their net charge. Whereas the conformation in the C-terminal pentapeptide has been shown to be of importance at the Y_5 and Y_4 receptors (but is probably also of high impact at the other receptors), the present work indicates that features of the N-terminal end of the helix are also of importance. Indeed, the observed structural differences between the wild-type peptides and their chimeras are minor and cannot fully account for the dramatic changes in their pharmacology. To which relative extent structural or electrostatic effects may trigger larger differences in binding to their receptors can only be answered when more reliable models of the structural features of the corresponding ligand−receptor complexes become available. Presently, work is in progress in our laboratory to create functional models for the Y receptors in order to study such features more directly.

ACKNOWLEDGMENT

We would like to especially acknowledge Bruker Biospin AG, Fällanden, for generously allowing us to access their Avance 700 MHz NMR spectrometer and Dr. R. Kümmerle for helping setting up the experiments. We would like to thank Dr. T. Kohno for providing us the plasmid for the ubiquitin fusion vector and Prof. J. A. Robinson and Dr. A. Renard for help during the peptide synthesis and for access to their SPPS robot. We are also grateful to the referees for very useful comments.

SUPPORTING INFORMATION AVAILABLE

Tables of chemical shifts, $^{15}N\{^1H\}$-NOE data in solution and in the presence of micelles, plus information on the structure calculations. This material is available free of charge via the Internet at http://pubs.acs.org.

REFERENCES

1. Michel, M. C., Beck-Sickinger, A., Cox, H., Doods, H. N., Herzog, H., Larhammar, D., Quirion, R., Schwartz, T., and Westfall, T. (1998) XVI. International Union of Pharmacology recommendations for the nomenclature of neuropeptide Y, peptide YY, and pancreatic polypeptide receptors, *Pharmacol. Rev. 50*, 143−150.
2. Schwartz TW, T. H. (1981) Isolation and biogenesis of a new peptide from pancreatic islets, *Nature 294*, 589−591.
3. Hazelwood, R. L. (1993) The pancreatic polypeptide (PP-fold) family: gastrointestinal, vascular, and feeding behavioral implications, *Proc. Soc. Exp. Biol. Med. 202*, 44−63.
4. Mörl, K., and Beck-Sickinger, A. G. (2004) Structure-activity relationship of peptide-derived ligands at Y-receptors, in *Handbook of Experimental Pharmacology* (Michel, M. C., Ed.) Vol. 162, pp 480−503, Springer Verlag, Berlin.
5. Cabrele, C., Wieland, H. A., Langer, M., Stidsen, C. E., and Beck-Sickinger, A. G. (2001) Y-receptor affinity modulation by the design of pancreatic polypeptide/neuropeptide Y chimera led to Y5-receptor ligands with picomolar affinity, *Peptides 22*, 365−378.
6. Cabrele, C., and Beck-Sickinger, A. G. (2000) Molecular characterization of the ligand−receptor interaction of the neuropeptide Y family, *J. Pept. Sci. 6*, 97−122.
7. Blundell, T. L., Pitts, J. E., Tickle, I. J., Wood, S. P., and Wu, C.-W. (1981) X-ray analysis (1.4 Å resolution) of avian pancreatic polypeptide: Small globular protein hormone, *Proc. Natl Acad. Sci. U.S.A. 78*, 4175−4179.
8. Li, X. A., Sutcliffe, M. J., Schwartz, T. W., and Dobson, C. M. (1992) Sequence-specific ^1H NMR assignments and solution structure of bovine pancreatic polypeptide, *Biochemistry 31*, 1245−1253.
9. Darbon, H., Bernassau, J. M., Deleuze, C., Chenu, J., Roussel, A., and Cambillau, C. (1992) Solution conformation of human neuropeptide Y by ^1H nuclear magnetic resonance and restrained molecular dynamics, *Eur. J. Biochem. 209*, 765−771.
10. Monks, S. A., Karagianis, G., Howlett, G. J., and Norton, R. S. (1996) Solution structure of human neuropeptide Y, *J. Biomol. NMR 8*, 379−390.
11. Cowley, D. J., Hoflack, J. M., Pelton, J. T., and Saudek, V. (1992) Structure of neuropeptide Y dimer in solution, *Eur. J. Biochem. 205*, 1099−1106.
12. Bader, R., Bettio, A., Beck-Sickinger, A. G., and Zerbe, O. (2001) Structure and dynamics of micelle-bound neuropeptide Y: com-

parison with unligated NPY and implications for receptor selection, *J. Mol. Biol. 305*, 307−329.
13. Kaiser, E. T., and Kezdy, F. J. (1984) Amphiphilic secondary structure: design of peptide hormones, *Science 223*, 249−255.
14. Sargent, D. F., and Schwyzer, R. (1986) Membrane lipid phase as catalyst for peptide-receptor interactions, *Proc. Natl Acad. Sci. U.S.A. 83*, 5774−5778.
15. Schwyzer, R. (1986) Molecular mechanism of opioid receptor selection, *Biochemistry 25*, 6335−6342.
16. Moroder, L., Romano, R., Guba, W., Mierke, D. F., Kessler, H., Delporte, C., Winand, J., and Christophe, J. (1993) New evidence for a membrane-bound pathway in hormone receptor binding, *Biochemistry 32*, 13551−13559.
17. Bader, R., Rytz, G., Lerch, M., Beck-Sickinger, A. G., and Zerbe, O. (2002) Key motif to gain selectivity at the neuropeptide Y5-receptor: structure and dynamics of micelle-bound [Ala^{31}, Pro^{32}]-NPY, *Biochemistry 41*, 8031−8042.
18. Lerch, M., Gafner, V., Bader, R., Christen, B., Folkers, G., and Zerbe, O. (2002) Bovine pancreatic polypeptide (bPP) undergoes significant changes in conformation and dynamics upon binding to DPC micelles, *J. Mol. Biol. 322*, 1117−1133.
19. Lerch, M., Mayrhofer, M., and Zerbe, O. (2004) Structural similarities of micelle-bound peptide YY (PYY) and neuropeptide Y (NPY) are related to their affinity profiles at the Y receptors, *J. Mol. Biol. 339*, 1153−1168.
20. Kohno, T., Kusunoki, H., Sato, K., and Wakamatsu, K. (1998) A new general method for the biosynthesis of stable isotope-enriched peptides using a decahistidine-tagged ubiquitin fusion system: an application to the production of mastoparan-X uniformly enriched with ^{15}N and $^{15}N/^{13}C$, *J. Biomol. NMR 12*, 109−121.
21. Güntert, P., Mumenthaler, C., and Wüthrich, K. (1997) Torsion angle dynamics for NMR structure calculation with the new program DYANA, *J. Mol. Biol. 273*, 283−298.
22. Laskowski, R. A., Rullmannn, J. A., MacArthur, M. W., Kaptein, R., and Thornton, J. M. (1996) AQUA and PROCHECK-NMR: programs for checking the quality of protein structures solved by NMR, *J. Biomol. NMR 8*, 477−486.
23. Koradi, R., Billeter, M., and Wüthrich, K. (1996) MOLMOL: a program for display and analysis of macromolecular structures, *J. Mol. Graphics 14*, 51−55, 29−32.
24. Lee, T. H., Mozsolits, H., and Aguilar, M. I. (2001) Measurement of the affinity of melittin for zwitterionic and anionic membranes using immobilized lipid biosensors, *J. Pept. Res. 58*, 464−476.
25. Mozsolits, H., and Aguilar, M. I. (2002) Surface plasmon resonance spectroscopy: an emerging tool for the study of peptide-membrane interactions, *Biopolymers 66*, 3−18.
26. Killian, J. A., and von Heijne, G. (2000) How proteins adapt to a membrane-water interface, *Trends Biochem. Sci. 25*, 429−434.
27. Engelman, D. M., Chen, Y., Chin, C. N., Curran, A. R., Dixon, A. M., Dupuy, A. D., Lee, A. S., Lehnert, U., Matthews, E. E., Reshetnyak, Y. K., Senes, A., and Popot, J. L. (2003) Membrane protein folding: beyond the two stage model, *FEBS Lett. 555*, 122−125.
28. Chou, P. Y., and Fasman, G. D. (1078) Empirical predictions of protein conformation, *Annu. Rev. Biochem. 47*, 251−276.
29. Piserchio, A., Shimizu, N., Gardella, T. J., and Mierke, D. F. (2002) Residue 19 of the parathyroid hormone: structural consequences, *Biochemistry 41*, 13217−13223.
30. Bechinger, B. (1996) Towards membrane protein design: pH-sensitive topology of histidine-containing polypeptides, *J. Mol. Biol. 263*, 768−775
31. Ladokhin, A. S., and White, S. H. (2004) Interfacial folding and membrane insertion of a designed helical peptide, *Biochemistry 43*, 5782−5791.
32. Wimley, W. C., and White, S. H. (1996) Experimentally determined hydrophobicity scale for proteins at membrane interfaces, *Nat. Struct. Biol. 3*, 842−848.
33. Beck-Sickinger, A. G., Wieland, H. A., Wittneben, H., Willim, K. D., Rudolf, K., and Jung, G. (1994) Complete L-alanine scan of neuropeptide Y reveals ligands binding to Y_1 and Y_2 receptors with distinguished conformations, *Eur. J. Biochem. 225*, 947−958.
34. Gehlert, D. R., Schober, D. A., Beavers, L., Gadski, R., Hoffman, J. A., Smiley, D. L., Chance, R. E., Lundell, I., and Larhammar, D. (1996) Characterization of the peptide binding requirements for the cloned human pancreatic polypeptide-preferring receptor, *Mol. Pharmacol. 50*, 112−118.
35. Gingerich, R. L., Akpan, J. O., Gilbert, W. R., Leith, K. M., Hoffmann, J. A., and Chance, R. E. (1991) Structural requirements of pancreatic polypeptide receptor binding, *Am. J. Physiol. 261*, 319−324.
36. Walker, P., Munoz, M., Martinez, R., and Peitsch, M. C. (1994) Acidic residues in extracellular loops of the human Y_1 neuropeptide Y receptor are essential for ligand binding, *J. Biol. Chem. 269*, 2863−2869.
37. Eckard, C. P., Cabrele, C., Wieland, H. A., and Beck-Sickinger, A. G. (2001) Characterisation of neuropeptide Y receptor subtypes by synthetic analogues and by anti-receptor antibodies, *Molecules 6*, 448−467.
38. Bettio, A., Dinger, M. C., and Beck-Sickinger, A. G. (2002) The neuropeptide Y monomer in solution is not folded in the pancreatic-polypeptide fold, *Protein Sci. 11*, 1834−1844.
39. McCrea, K., Wisialowski, T., Cabrele, C., Church, B., Beck-Sickinger, A. G., Kraegen, E., and Herzog, H. (2000) 2-36[K4,-RYYSA(19-23)]PP a novel Y5-receptor preferring ligand with strong stimulatory effect on food intake, *Regul. Pept. 87*, 47−58.

BI0501232